Boundary-Layer Meteorol (2016) 161:1–17
DOI 10.1007/s10546-016-0161-x

RESEARCH ARTICLE

Exploring Eddy-Covariance Measurements Using a Spatial Approach: The Eddy Matrix

Christian Engelmann[1,2] · **Christian Bernhofer**[1]

Received: 25 August 2015 / Accepted: 5 April 2016 / Published online: 22 April 2016

Abstract Taylor's frozen turbulence hypothesis states that "standard" eddy-covariance measurements of fluxes at a fixed location can replace a spatial ensemble of instantaneous values at multiple locations. For testing this hypothesis, a unique turbulence measurement set-up was used for two measurement campaigns over desert (Namibia) and grassland (Germany) in 2012. This "Eddy Matrix" combined nine ultrasonic anemometer–thermometers and 17 thermocouples in a 10 m × 10 m regular grid with 2.5-m grid distance. The instantaneous buoyancy flux derived from the spatial eddy covariance of the Eddy Matrix was highly variable in time (from −0.3 to 1 m K s^{-1}). However, the 10-min average reflected 83 % of the reference eddy-covariance flux with a good correlation. By introducing a combined eddy-covariance method (the spatial eddy covariance plus the additional flux of the temporal eddy covariance of the spatial mean values), the mean flux increases by 9 % relative to the eddy-covariance reference. Considering the typical underestimation of fluxes by the standard eddy-covariance method, this is seen as an improvement. Within the limits of the Eddy Matrix, Taylor's hypothesis is supported by the results.

Keywords Buoyancy flux · Eddy covariance · Spatial covariance · Taylor's hypothesis

1 Introduction

Taylor's frozen turbulence hypothesis (Taylor 1938) is a pre-requisite for standard surface flux measurements based on the eddy-covariance (EC) method (Stull 1988). It allows one to replace a spatial ensemble of instantaneous values at multiple locations with a sufficiently

✉ Christian Engelmann
christian.engelmann@tu-dresden.de

1 Chair of Meteorology, Institute of Hydrology and Meteorology, Technische Universität Dresden, Pienner Str. 23, 01737 Tharandt, Germany

2 Present Address: Institute for Groundwater Management, Technische Universität Dresden, Bergstr. 66, 01062 Dresden, Germany

long temporal record at one location. Despite its crucial importance, only a few studies have investigated the validity of Taylor's hypothesis. For instance, Mauder et al. (2008) used a large spatial set-up and observed systematically higher sensible heat flux H in comparison with solely time-averaged data based on the EC technique. Christen and Vogt (2004) analyzed dispersive fluxes (probably caused by low-frequency turbulent organized structures; see, e.g., Kanda et al. 2004) in a sparse canopy. In their study eight irregularly installed ultrasonic anemometer–thermometers (referred to as "ultrasonic" hereafter) demonstrated that up to 15 % of the total momentum flux resulted from dispersive fluxes, but no significant changes in H values were found. Katul et al. (1999) investigated the spatial variability of turbulence statistics using seven single towers above a pine forest that were horizontally separated by distances of at least 100 m. It was found that the sensible heat flux was relatively spatially homogeneous (variation coefficient $\approx$17 %) compared with the fluxes of latent heat and carbon dioxide. Mahrt et al. (2009) investigated space-time statistics for mesoscale motions under stable atmospheric conditions and found that the spatial coherence depended on the averaging time and also on the synoptic regime and on the type of underlying surface. Obviously, the general applicability of Taylor's hypothesis under atmospheric field conditions are not yet completely clear. It is assumed that eddies are ergodic (and therefore behave according to Taylor's hypothesis) when they have sizes that are smaller than the height of the boundary layer and temporal scales of less than 30 min (Chen et al. 2014). However, this assumption is based on a few experiments and cannot be generalized. Thomas et al. (2012) determined spatial patterns of sensible heat fluxes with a fibre-optics set-up and found that during stable stratification, Taylor's hypothesis was not valid.

In this study, an attempt is made to map a sub-sample of the spatial variability of the turbulent values of the atmosphere using a specific set-up of instruments, the "Eddy Matrix", in two measurement campaigns over desert (Namibia) and grassland (Germany). Eddy Matrix data are used for a comparison of spatially-averaged instantaneous fluxes and fluxes calculated via standard temporal EC methods to meet the objective of exploring differences due to potential violations of Taylor's hypothesis. To our knowledge, this is the first experimental attempt to investigate Taylor's hypothesis, and it has important potential consequences, e.g., for the homogeneity requirements (e.g., Raupach and Shaw 1982; Panin et al. 1998; Aubinet et al. 2012) or the often-discussed energy budget closure problem (e.g., Desjardins et al. 1992; Mahrt 1998; Twine et al. 2000; Wilson et al. 2002; Oncley et al. 2007; Foken 2008a; Stoy et al. 2013).

The study therefore has the following objectives: (i) to test Taylor's hypothesis by comparing the temporal and spatial EC methods for these experiments and (ii) to demonstrate the associated measurement challenges and potentially resulting benefits for the derived fluxes.

2 Material

2.1 Sites

The Gobabeb Research and Training Centre (23°52′S, 15°09′E) is located in Western Namibia (east of Walvis Bay and approximately 60 km from the coast) in a desert environment. The measurements were performed between August 16 and August 23. 2012 almost at the centre of a level area of approximately 4.5 km^2 and approximately 1.2 km north-east of the Gobabeb Research and Training Centre (Fig. 1a). The immediate surroundings of the experimental field were largely homogeneous and practically without vegetation. The surface slope in all spatial

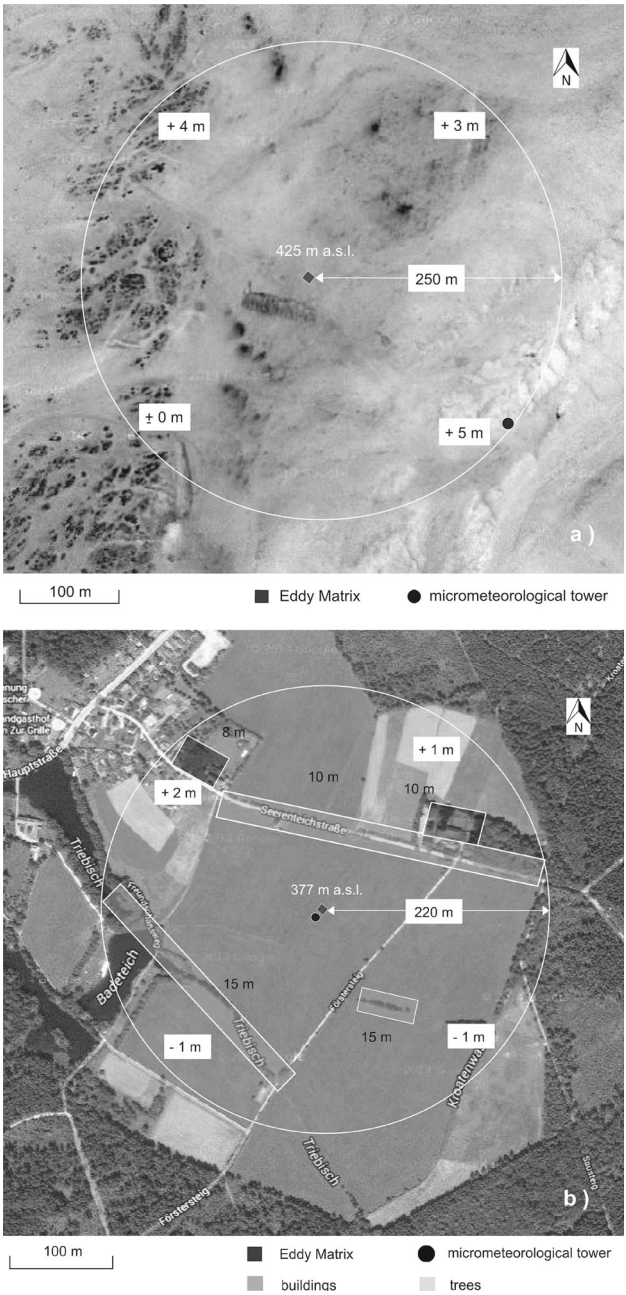

Fig. 1 Measurement locations and fetch requirements (background images: Google Maps, 2013): **a** at Go babeb, dark textures are bare rocks or small ditches, and **b** at Grillenburg, including certain roughness elements. The altitude refers to the Eddy Matrix at the centre. The radius of the area around the measurement location represents the required fetch, assuming a ratio between the measurement height (above the zero-plane displacement) and fetch of 1/100. The *numbers* in the *white boxes*indicate relative altitude changes in each direction

directions is flat, with gradients ranging between 0.6 and 1.8 %, running from the north-east to the south-west. A continuously operating micrometeorological tower (with instruments from the University of Basel, Switzerland and the Karlsruhe Institute of Technology, KIT, Karlsruhe, Germany) is located approximately 270 m south-east of the measurement location.

The station at Grillenburg, Germany (operated by the Chair of Meteorology, TU Dresden), was chosen to test the set-up and methodology before shipping the instruments to Namibia. The site is located in the lower regions of the Ore Mountains (50°57′N, 13°31′E) at an altitude of 385 m a.s.l., situated on a 0.4 km^2 clearing in the Tharandter Wald (Fig. 1b). As part of the European greenhouse gas monitoring system (ICOS-D, the German contribution to Integrated Carbon Observation System at European level), it provides a standardized determination of the vertical fluxes over ecosystems (Prescher et al. 2010). The site is flat and characterized by continuous grass cover, which is mowed several times per year, while mixed stands of spruce and pine surround the extended meadow. The grass height was approximately 0.45 m at the time of the measurement campaign between May 10 and May 16. 2012. The approximate size of the estimated necessary fetch is 220 m. The surface slope has gradients ranging between 0.5 and 0.7 %, running from the north-west to the south-east. The fetch is influenced by several roughness elements (lines of deciduous trees and two residential buildings). Immediately at the south-western edge of the measuring field is the fenced area of the Grillenburg station. It can be assumed that the station itself has an influence on the formation of turbulence within the measuring field. These site limitations have to be taken into account when considering the results.

2.2 Measurement Set-up

The set-up covered a horizontal area of 10 m × 10 m (Fig. 2) using a total of nine ultrasonics (model 81000, R.M. Young Company, Michigan, USA), which were separated by a perpendicular distance of 5 m. The measurement height of the ultrasonics was 2.5 m above ground. Each ultrasonic was aligned carefully vertically and to the north. Because of its schematic design, the set-up was named the “Eddy Matrix”. Before both campaigns, an inter-calibration

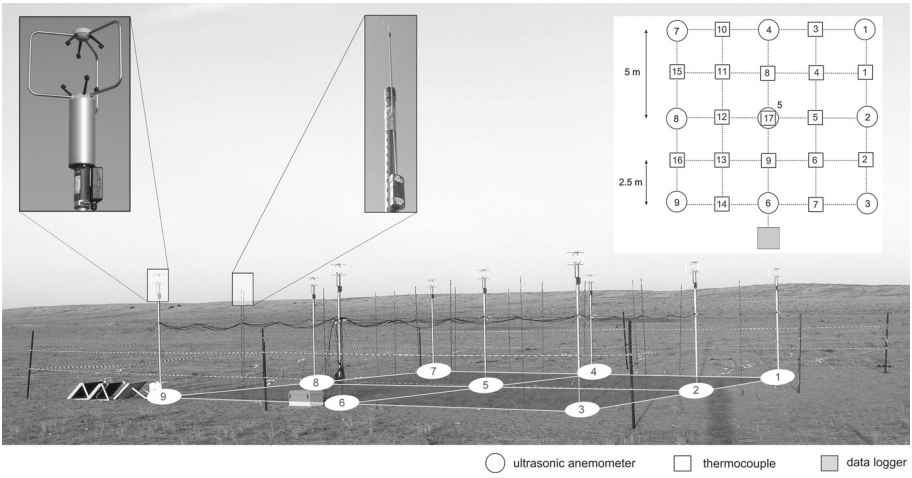

Fig. 2 Measurement set-up in Gobabeb as viewed when facing east. The *numbers* represent individual sensors

was done for all ultrasonics for a period of approximately 1 week. Additionally, a total of 17 thermocouples (based on TEEB-2 type E, Campbell Scientific Inc., Utah, USA) were placed in the already-constructed measurement matrix for additional analysis of the spatial turbulence. They were aligned with each other and the ultrasonics with a perpendicular separation of 2.5 m and at the same height as the ultrasonics. One thermocouple was placed adjacent to the central ultrasonic for a redundant measurement of air temperature.

The measurement data were stored on three data loggers (model CR1000, Campbell Scientific Inc., UT, USA) as raw data. An automatic synchronization of loggers 2 and 3 with logger 1 was performed every 3 h, resulting a maximum deviation of 0.06 s per synchronization interval. Additionally, the net radiation R_n (Gobabeb: model CNR4, Kipp & Zonen, Germany; Grillenburg: model CNR1, Kipp & Zonen, Germany), soil heat flux G (Gobabeb: model HTF3, Campbell Scientific Inc., Utah, USA; Grillenburg: model LWS, PLE Laborelektronik, Austria) and water vapour concentration c_{H_2O} (Grillenburg: model LI-7000, LI-COR Biosciences GmbH, Germany) were obtained for determining the latent heat flux LE in combination with an additional ultrasonic. These were used to quantify the measurement conditions and to estimate the available energy ($R_n - G$). The R_n and G data for Gobabeb were provided by the University of Basel.

2.3 Measurement Conditions

Gobabeb provided excellent measurement conditions, with a series of almost ideal radiation days (Fig. 3a). At night, minimum temperatures of approximately 7 °C, increasing to 28 °C during the day, were measured. Relatively low values of R_n were observed due to high surface temperatures and low albedo. The sensible heat flux H achieved values of 0.5–0.8 R_n during daytime. Fog occurred in the morning hours of August 19 and 20, causing some deposition at the instruments. The atmospheric stratification was mostly unstable during daytime and near-neutral or stable at night.

At Grillenburg, the weather was far more variable (Fig. 3b). Air temperatures reached a maximum of 29 °C on May 11, subsequently followed by a thunderstorm event and cooler weather. During the thunderstorm, rainfall with a maximum intensity of 8 mm per 10 min occurred. R_n reached typical values of approximately 600 W m^{-2} at noon and H only maximum values of up to 200 W m^{-2} due to evapotranspiration. For most of the experiment, near-neutral atmospheric stratification was present, with very short unstable periods during daytime. Very stable periods rarely occurred at night.

3 Methods

3.1 Data Preparation

First, the raw data, the acoustic air temperature θ and the wind-speed components in all spatial directions, v_x, v_y and v_z (= w), were checked for implausible values (Table 1), and these points in time were disregarded in the analyzes. Additionally, de-spiking was performed according to Aubinet et al. (2012) using a fixed discrimination factor of 5. For pragmatic reasons of comparability between the individual 10-min periods, certain 10-min periods were excluded based on the following criteria: a ratio of filtered values >1 % or a number of data points <90 % of the maximum number. When separating the data based on the atmospheric stability, the stability classification of Tillman (1972) was used (unstable: $-0.2 < \zeta < 0$, free convection: $-\infty < \zeta \leq -0.2$, stable: $0 \leq \zeta < \infty$; ζ is the stability parameter).

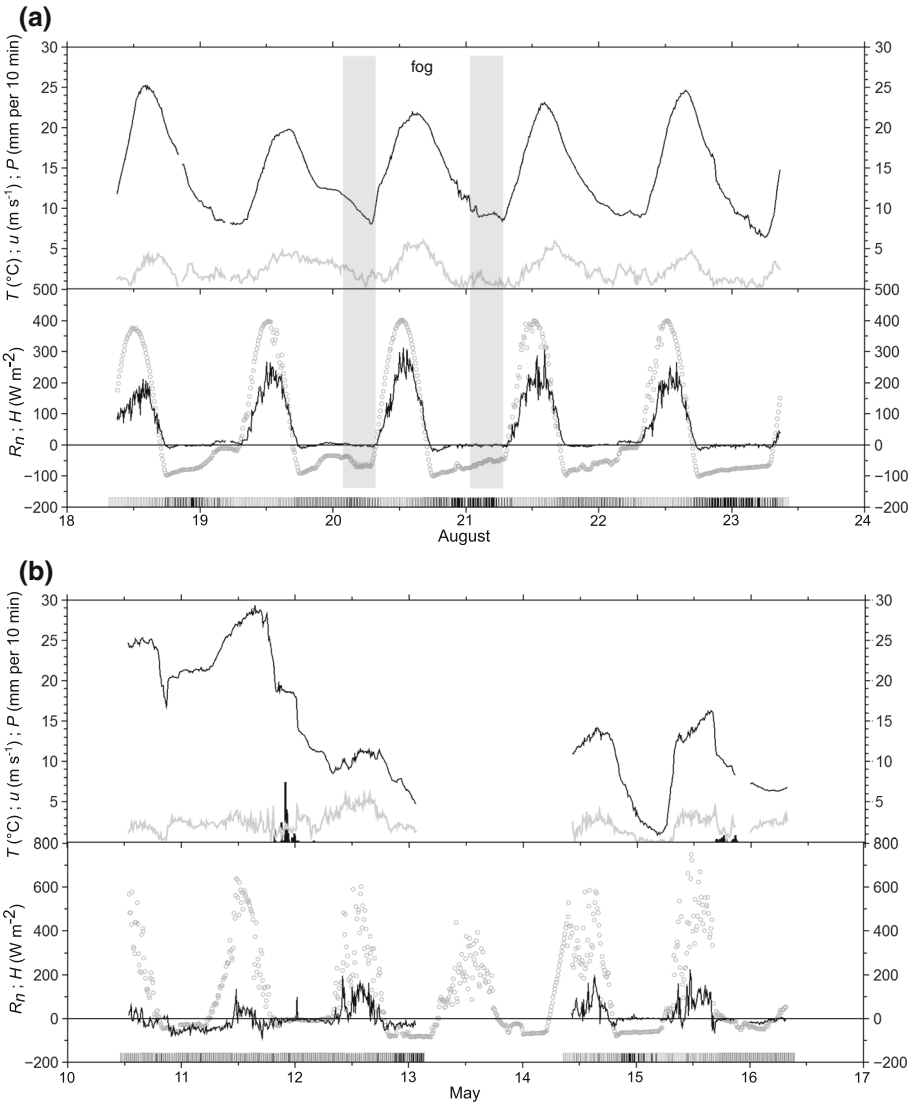

Fig. 3 Measurement conditions at **a** Gobabeb and **b** Grillenburg. *Top* mean acoustic air temperature (ultrasonic 5, *black*), wind velocity (ultrasonic 5, *light gray*), precipitation (*bold black*). *Bottom* net radiation R_n (*circles*) and sensible heat flux H (*black*) derived by the temporal EC method (ultrasonic 5). Additionally, periods with fog and the atmospheric stability (stable: *black*, near-neutral: *dark gray*, unstable: *light grey*) are indicated. In **b**, the first gap is due to an intentional shut-down before a thunderstorm, the second one is caused by data filtering (plausibility, de-spiking)

Because of the inevitable erroneous vertical orientation of the ultrasonics and the inclined ground surface, a tilt correction must be performed. Here, a two-dimensional rotation was used to align the resulting wind vector relative to the streamlines (McMillen 1988). An analysis of the angles after double rotation indicated that the vertical alignment of the ultrasonics was very good, with vertical angles of less than 4° for both sites. The double-rotated raw flux data were used for the temporal EC method. However, for the spatial EC method, theoretically we need to correct for the erroneous instantaneous vertical wind speed resulting from misalignment

Table 1 Mean sensor accuracies as well as value ranges, which were used used for plausibility testing

Variable	Unit	Accuracy	Min	Max
θ	°C	± 2	−5	35
v_x	m s^{-1}	±0.05	−30	30
v_y	m s^{-}1	±0.05	−30	30
v_z	m s^{-1}	±0.05	−5	5

of each ultrasonic. To remove at least the calibration offset, the mean vertical wind speed measured by each ultrasonic was calculated over the entire measurement period, and the deviation from zero was subtracted from each ultrasonic's raw data value (i.e., mean removal was performed). Mean vertical wind speeds of approximately −0.10 and −0.28 m s^{-1} were measured at Gobabeb and Grillenburg, respectively, with little differences among individual ultrasonics. The resulting fluxes of all different treatments of rotation indicated that the differences between no tilt correction, double rotation and mean removal were negligible. However, mean removal was used for the spatial EC method to avoid systematic biases due to offsets in w.

3.2 Temporal EC Method

To determine the sensible heat flux H, the temporal or classical EC method first calculates the buoyancy flux B_t (which is also referred to as the sonic-derived buoyancy flux; Liu et al. 2001) by performing a covariance based on a Reynolds decomposition (Reynolds 1895), where t indicates "temporal" (e.g., Foken 2008b),

$$B_t = \overline{w'\theta'} \tag{1a}$$

$$= \left(\frac{1}{M-1}\right) \sum_{i=1}^{M} \left(\left(w_i - \overline{w}\right) \left(\theta_i - \overline{\theta}\right) \right), \tag{1b}$$

where the overbar denotes an average over a time period, typically of 10 to 60 min, and M is the number of measurements in the interval (for 10 min and 10 Hz, $M = 6000$). All temporal averaging was performed for 10-min intervals.

3.3 Spatial EC Method

An ensemble mean based on the Eddy Matrix was used to calculate a spatial eddy covariance to determine the buoyancy flux B_a, where a represents "areal",

$$B_a = \left\langle w''\theta'' \right\rangle \tag{2a}$$

$$= \left(\frac{1}{N-1}\right) \sum_{j=1}^{N} \left(\left(w_j - \langle w \rangle\right) \left(\theta_j - \langle \theta \rangle\right) \right), \tag{2b}$$

where $\langle\rangle$ denotes a spatial mean, and N is the number of measurement points (in our case, nine ultrasonics in the Eddy Matrix). For such small samples, it is particularly important to decide whether to divide by $(N - 1)$ or by N. Here, we want to approximate the statistical population. Therefore, the unbiased covariance is used, as is the case in many works, e.g., Foken (2008b). To match both the temporal and spatial covariances, the instantaneous values of B_a were temporally averaged to yield $\overline{B_a}$ with an interval of 10 min. This spatial flux

approach $\overline{B_a}$ is somewhat analogous to the method of Christen and Vogt (2004), who studied dispersive fluxes in a sparse canopy.

3.4 Combined EC Method

A third approach adds the temporal eddy covariance of the spatial mean values of the Eddy Matrix (right term) to the mean of the spatial eddy covariance to account for the limited spatial coverage of the Eddy Matrix, both over the standard averaging time of 10 min,

$$B_{\text{comb}} = \overline{\langle w''\theta'' \rangle} + \overline{\langle w \rangle' \langle \theta \rangle'} \tag{3a}$$

$$= \overline{B_a} + \left(\frac{1}{M-1} \right) \sum_{i=1}^{M} \left(\left(\langle w \rangle_i - \overline{\langle w \rangle} \right) \left(\langle \theta \rangle_i - \overline{\langle \theta \rangle} \right) \right), \tag{3b}$$

where the overbar denotes the temporal mean and $\langle\rangle$ denotes the spatial mean. The right term in Eq. 3 adds information about the entire Eddy Matrix set-up (larger acquisition area than a single sensor) and might collect information about larger-scale structures moving slower than small eddies. However, this is an assumption that has to be proven in further work.

3.5 Deriving Characteristic Sensible Heat Fluxes

For a first comparison with energy balance components, sensible heat fluxes H were derived from B_t. Standard corrections were applied (see, e.g., Liu et al. 2001). Because no directly measured latent flux was available for transforming acoustic into potential temperatures at Gobabeb, the humidity correction of Schotanus et al. (1983) was adapted (Frühauf 1998),

$$H = \overline{\rho} c_p \frac{B_t - 0.51\,\overline{\theta}\ (R_n - G)\ \ (\overline{\rho} L)^{-1}}{1 - 0.51 \frac{c_p\,\overline{\theta}}{L}}, \tag{4}$$

where storage components are ignored. At Gobabeb, the mean G and R_n were stored only at 30-min intervals; thus, the values of each interval were assumed to be constant to yield 10-min-averaged values of $(R_n - G)$. The mean air density $\overline{\rho}$ and specific heat capacity of air at constant pressure c_p were set to constant values ($\overline{\rho} \approx 1.2$ kg m^{-3}, representing 15 °C, and $c_p = 1005$ J kg^{-1} K^{-1}) for reasons of simplicity. The Obukhov length L was calculated using the temporal EC method. Also, a spectral correction (Moore 1986) was performed. Generally, it would be imaginable to insert $\overline{B_a}$ or B_{comb} instead of B_t. However, the validity of Eq. 4 has to be proven in this case, but this is not the focus here.

4 Results

4.1 Temporal EC Method

The results of the temporal EC method from all nine ultrasonics within the Eddy Matrix are compared in Table 2. Using the central ultrasonic as a reference, very good correlations ($R^2 > 0.9$) were obtained for both sites for unstable conditions. ultrasonic instrument 7 measured very similar fluxes despite its higher sensitivity to spikes. The relatively poor correlations of ultrasonics 6, 8 and 9 (a and $R^2 \leq 0.8$) during stable conditions at Gobabeb are not fully understood. We assume this might be associated to the solar panels and the logger box, which were upstream of ultrasonics 6, 8 and 9 during most of the experiment (see

Table 2 Intercomparison between the buoyancy fluxes B_t yielded by each ultrasonic

Ultrasonic	Gobabeb				Grillenburg			
	Stable		Unstable		Stable		Unstable	
	a	R^2	a	R^2	a	R^2	a	R^2
1	1.02	0.80	1.02	0.94	1.00	0.89	1.09	0.83
2	0.94	0.89	0.97	0.96	0.94	0.92	1.00	0.85
3	0.96	0.84	0.97	0.93	0.92	0.90	1.00	0.87
4	0.87	0.91	0.97	0.93	0.96	0.91	0.98	0.88
6	0.70	0.73	0.94	0.92	0.96	0.91	0.90	0.89
7	0.92	0.89	0.98	0.93	0.98	0.90	1.01	0.86
8	0.74	0.81	0.97	0.96	1.01	0.91	0.94	0.87
9	0.80	0.79	0.96	0.92	0.99	0.90	0.90	0.84

The results are presented as linear regressions without offsets (slope a and coefficient of determination R^2) between each ultrasonic and the central one (no. 5)

Fig. 2). Obviously, the correlations are larger and the regression slope is closer to unity for unstable conditions than for stable ones. In general, all ultrasonics measured similar fluxes; thus, the central ultrasonic (no. 5) was used as the reference for further analysis.

4.2 Spatial Averaging

For illustration, specific time windows are shown at a high resolution (Figs. 4 and 5). A large range of values is observed for B_a in this relatively small spatial ensemble. During daytime, within a time period of 10 min, values between -0.3 and approximately 1 m K s^{-1} (representing instantaneous sensible heat fluxes of -400 to 1200 W m^{-2}) were measured, whereas typical 10-min temporal fluxes were between 0.1 and 0.2 m K s^{-1} (representing 120 to 240 W m^{-2}). Interesting turbulence structures and a corresponding reaction of B_a could be identified in daytime, especially for the temperature trace at Grillenburg. In contrast, these patterns are less pronounced for Gobabeb, but even stronger fluctuations in the temperature occurred. As expected, these variations were generally much less pronounced at night. Some special phenomena were observed: (i) sudden changes in the temperature trace were often accompanied by large variability in the instantaneous spatial fluxes, e.g., in Figs. 5a and 4b; (ii) despite almost-zero average nighttime fluxes, sometimes the instantaneous flux exhibited a clear increase in absolute magnitude, e.g., in Fig. 5b, which indicates (iii) non-steady-state conditions.

Next, diurnal courses were investigated based on the 10-min means of the spatial eddy covariances, in addition to the temporal and combined EC methods (Figs. 6a through 7b). The slopes of the regressions (calculated without offset) indicate that the spatial EC method only accounted for between 71 and 83 % of the reference B_t. The $\overline{B_a}$ values were, with some exceptions (especially at Grillenburg during nighttime), always slightly below B_t. In general, the differences between $\overline{B_a}$ and B_t (Figs. 6b and 7b) were small at night and maximal at noon, with underestimates of $\overline{B_a}$ of 0.05 and 0.03 m K s^{-1} at Gobabeb and Grillenburg, respectively.

The combined EC method B_{comb} resulted in higher daily values than B_t (Figs. 6 and 7). The correlations were also slightly improved: R^2 rose from 0.976 to 0.982 at Gobabeb and from 0.927 to 0.949 at Grillenburg. The regression slopes were improved from 0.83 to 1.09 and from 0.71 to 1.04, respectively. Thus, the combined EC method considerably increased the flux magnitude: (i) by 26 % at Gobabeb and by 33 % at Grillenburg compared with the averaged instantaneous spatial EC-method flux and (ii) by 9 % at Gobabeb and 4 % at Grillenburg compared with the temporal reference EC-method flux.

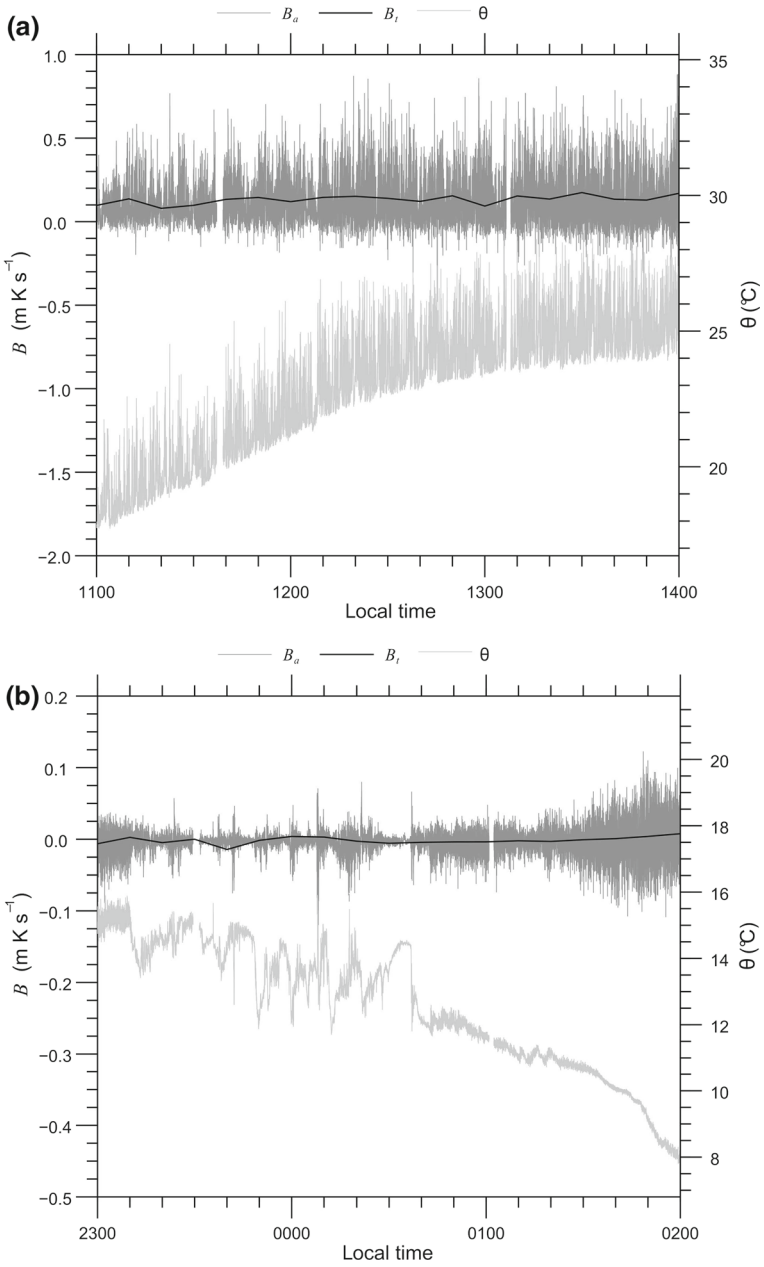

Fig. 4 Examples of 10-Hz data of B_a (*dark grey*, Eq. 2) and B_t (*black line*, ultrasonic 5, 10 min, Eq. 1) and θ (*light gray*, ultrasonic 5) at Gobabeb on August 18 during example hours at **a** day and **b** night. Note the different scales of the y axes in (**a**) and (**b**)

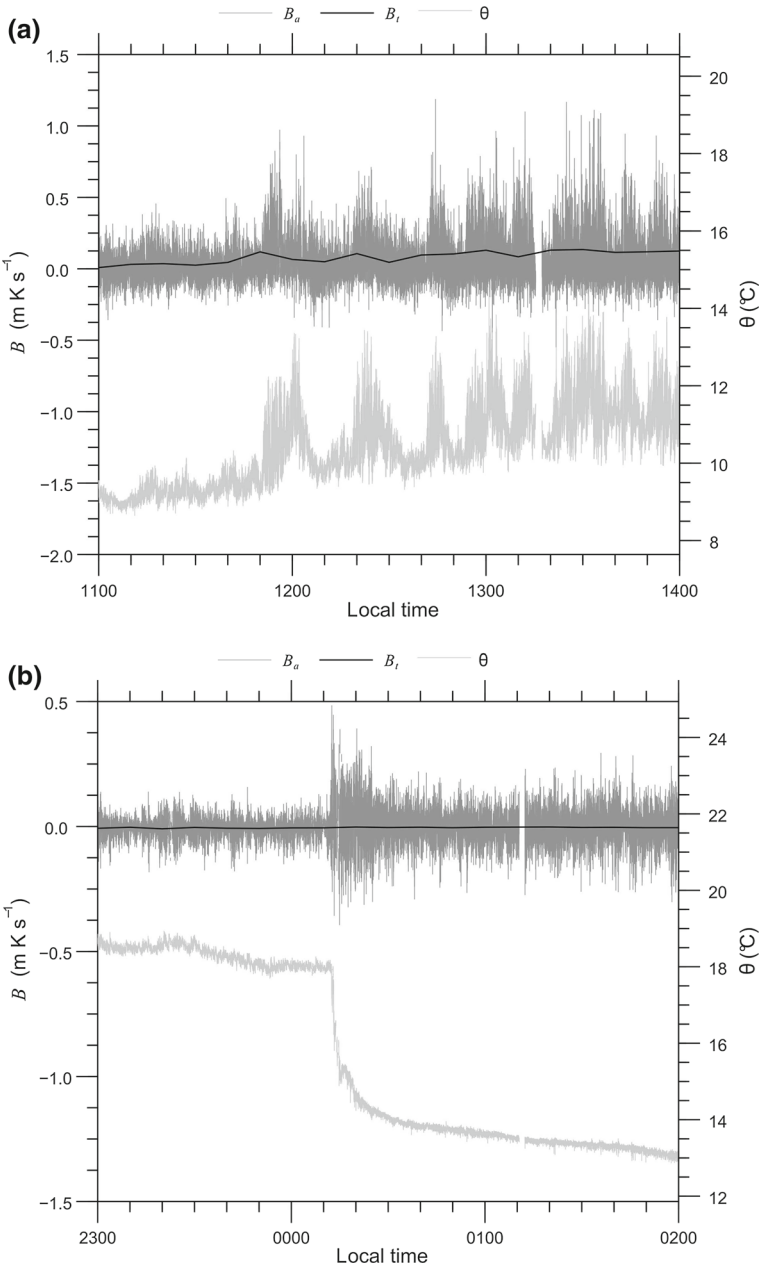

Fig. 5 Examples of 10-Hz data of B_a (*dark gray*, Eq. 2) and B_t (*black line*, ultrasonic 5, 10 min, Eq. 1) and θ (*light gray*, ultrasonic 5) at Grillenburg on May 12 during example hours at **a** day and **b** night. Note the different scales of the y axes in (**a**) and (**b**)

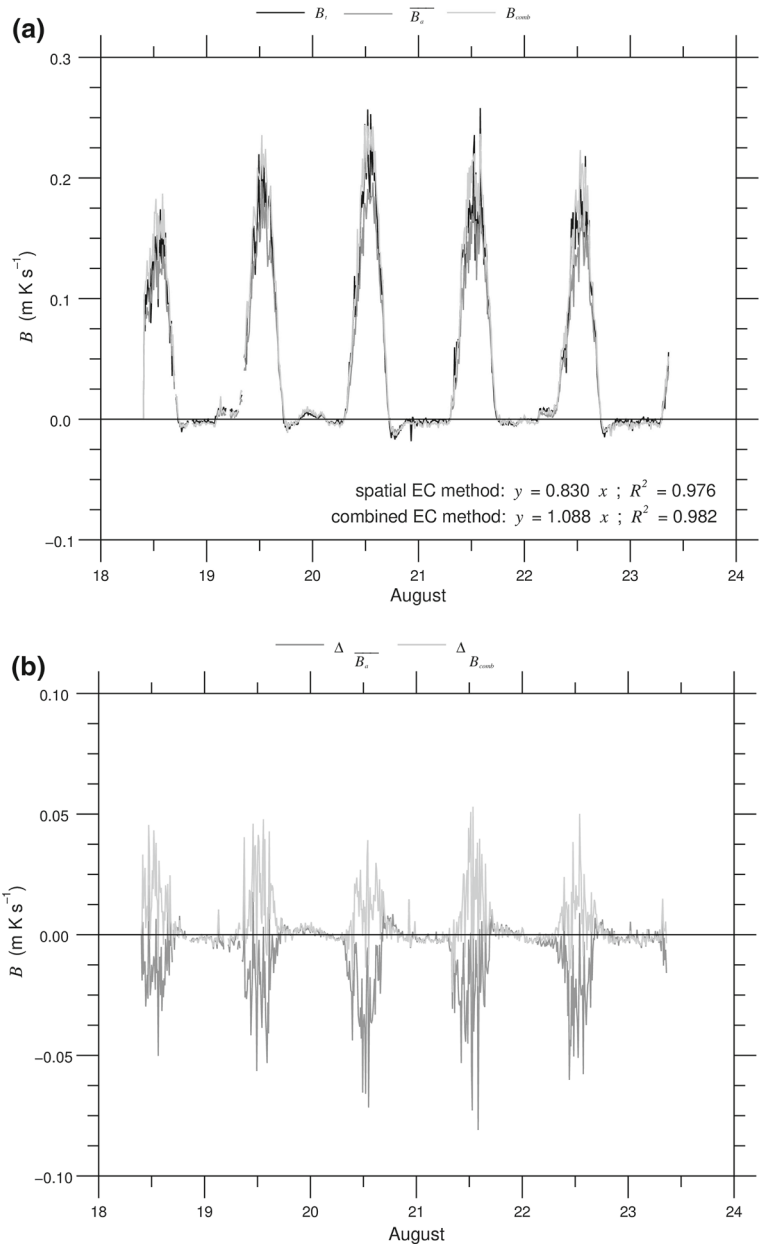

Fig. 6 **a** Diurnal courses of B_t (ultrasonic 5, 10 min, Eq. 1), $\overline{B_a}$ (10 min, Eq. 2) and B_{comb} (10 min, Eq. 3) at Gobabeb in addition to the results of the linear regressions without offset (slope a and coefficient of determination R^2) between the fluxes yielded by the spatial and temporal EC methods and the combined and temporal EC methods. The differences to the reference flux are shown in (**b**): Δ represents the difference between spatial and temporal fluxes and the difference between the combined and temporal buoyancy fluxes

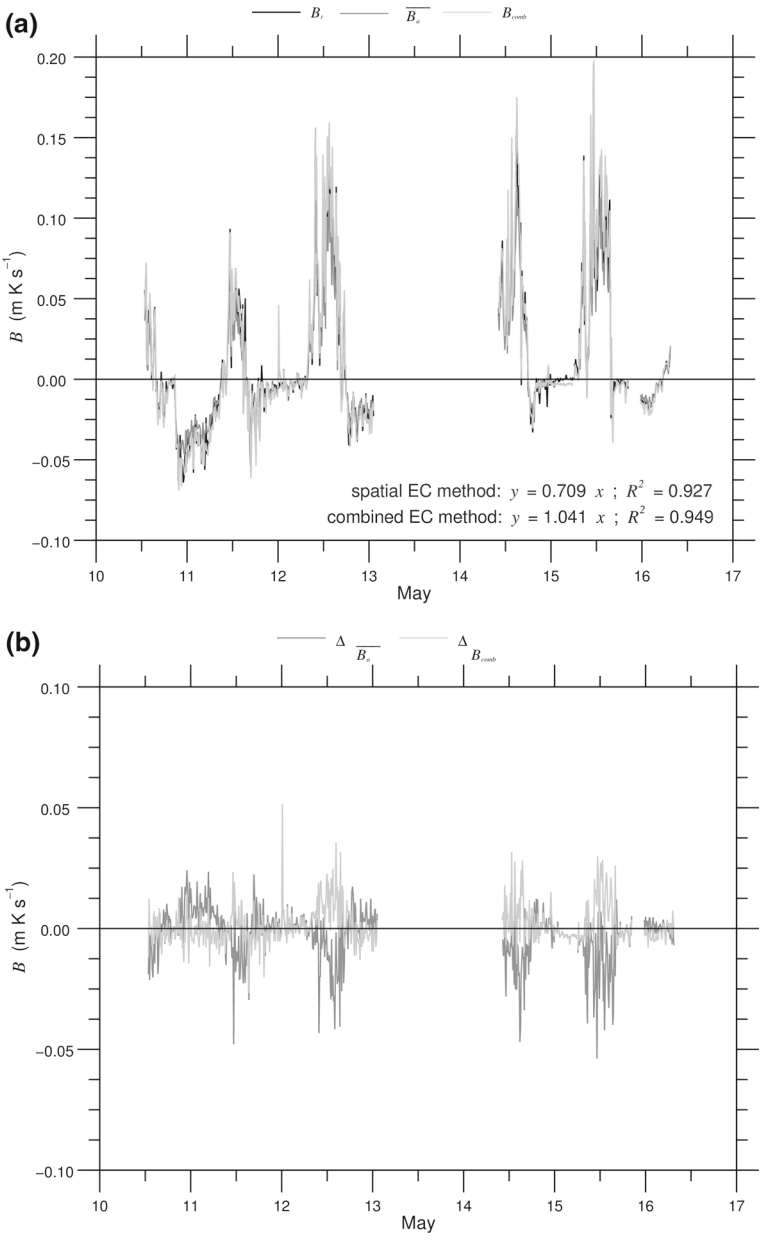

Fig. 7 **a** Diurnal courses of B_t (ultrasonic 5, 10 min, Eq. 1), $\overline{B_a}$ (10 min, Eq. 2) and B_{comb} (10 min, Eq. 3) at Grillenburg in addition to the results of the linear regressions without offset (slope a and coefficient of determination R^2) between the fluxes yielded by the spatial and temporal EC methods and the combined and temporal EC methods. The differences to the reference flux are shown in (**b**): Δ represents the difference between spatial and temporal fluxes and the difference between the combined and temporal buoyancy fluxes. In (b), the first gap is due to an intentional shut-down before a thunderstorm, the second one is caused by data filtering (plausibility, de-spiking)

5 Discussion

5.1 Buoyancy Flux

The spatial EC method theoretically requires coverage of a large area to arrive at a representative ensemble average. The Eddy Matrix represents only a small sub-sample. Therefore, the spatial covariances reach very high or low values during short periods, and averaging is needed for comparison with the temporal EC method. As expected, strong fluctuations in the high-resolution spatial covariance always coincide with larger values of friction velocity u_*, unstable stratification and relatively high values of R_n, which indicate convective exchange.

With the spatial EC method, however, additional information is collected, with the potential benefit of yielding additional flux contribution and for better understanding flux development. Consider the following illustration of the relationship between spatial and time integration: the spatial eddy covariance represents an averaging time, depending on the wind speed and size of the Eddy Matrix, whereas the temporal eddy covariance represents an area that depends on the wind speed and integration time. For example, at 1 m s^{-1} and an Eddy Matrix size of 10 m, we arrive at an integration time of 10 s for compatibility with the spatial fluxes. These fluxes still have a random characteristic, as indicated by the large fluctuations of the instantaneous spatial covariances. Averaging time was tested against the reference eddy covariances for different intervals between 1 and 60 min without changes above 10 min. Also, Foken (2008b) recommends an interval of 10–20 min for the EC method at sites with low measurement heights between 2 and 5 m for daytime unstable stratification. Therefore, the temporal integration of 10 min is used to arrive at representative fluxes.

With the combined EC method, the buoyancy fluxes could be increased considerably for Gobabeb and somewhat for Grillenburg, making them generally larger than temporal EC-method fluxes. Because the EC method typically underestimates turbulent fluxes (e.g., Wilson et al. 2002; Foken 2008b), the results of the combined EC method seem to be closer to reality than those of the temporal EC method for single sensors. Thus, we can assume that increasing the buoyancy flux (and consequently increasing the sensible heat flux) will yield an improved energy balance closure.

5.2 Testing Taylor's Hypothesis

Taylor's hypothesis is only investigated to a certain extent in this study. At a wind speed of 1 m s^{-1}, a turbulence structure would move completely through the Eddy Matrix and, assuming frozen turbulence, the first sensor would measure approximately the same pattern over time (in our case, 10 s) as all sensors along a line representing the wind direction. However, because the wind direction and speed can change rapidly, this concept is not complete. Strictly speaking, an air mass moving through the Eddy Matrix is a realization sampled at several locations (Aubinet et al. 2012). Steady-state conditions are by definition not needed for the spatial EC method because it represents an instantaneous value. However, a sample size of nine ultrasonics covering an area of only 10 m $\times$ 10 m, as in the Eddy Matrix, is small. Still, the Eddy Matrix provides additional information and consequently additional flux contribution. Thus the combined EC method, using the time average of the instantaneous spatial fluxes and the temporal eddy covariance from the spatial means of the instantaneous means of the Eddy Matrix, produces the highest absolute flux.

When comparing each individual ultrasonic to the reference, we observed horizontal variations in the temporally averaged buoyancy fluxes of the magnitude obtained by Katul et al. (1999) for a much larger set-up. Within the spatial limits of the Eddy Matrix, the time

means of the spatial fluxes agreed well with those of the standard temporal EC method. The increase in the absolute flux yielded by the combined method indicates the potential benefit of a multi-sensor set-up. This result might be in accordance with studies that include dispersive fluxes to yield a better spatial ensemble (Christen and Vogt 2004; Kanda et al. 2004; Mauder et al. 2008, 2010) and highlights the somewhat limited applicability of Taylor's hypothesis. Generally, according to Mahrt (2010), Taylor's hypothesis is valid when both the temporal and spatial scales are uniquely related. Mahrt (2010) points out that this assumption is not correct, at least for stable conditions, because "the submeso motions typically propagate faster than the mean flow".

6 Summary and Conclusions

A high-density matrix arrangement of EC instruments termed the Eddy Matrix was applied to investigate (i) the similarity of the results of the standard temporal EC method and those of the spatial EC method, and (ii) the measurement challenges and potentially resulting benefits for the derived fluxes. The study focused on the buoyancy flux and used nine ultrasonics in a 10 m $\times$ 10 m matrix over temperate grassland at the FLUXNET site Grillenburg, Germany and at Gobabeb, Namibia for approximately one week at each site.

The Eddy Matrix results indicated that approximately 83 and 71 % of the temporal flux at Gobabeb and Grillenburg, respectively, was accounted for by the instantaneous spatial flux for daytime conditions, but the flux could be increased to 109 and 104 % by utilizing the instantaneous spatial flux and the covariance of the spatial means of all nine ultrasonics in the combined method. Obviously, the flux is not completely covered by a single device. We speculate that this is due to coherent structures (Foken 2008b; Stoy et al. 2013) or not completely randomly organized turbulence. This would explain why the increase in fluxes was greater when the combined method was used at Gobabeb, where the homogeneous landscape is not as efficient at triggering larger-scale circulations as the relative heterogeneous landscape at Grillenburg. We assume that the ratio of measured eddies to the whole spectrum of all eddies is increased when a greater number of devices are used. It is surprising that the spatial extent of the Eddy Matrix was already sufficient to capture some additional flux because turbulent structures that are much larger than 10 m can occur. The differences between the fluxes derived by the three approaches show, that Taylor's hypothesis is obviously a reasonable assumption to conduct the temporal EC method at a fixed location. However, the results of the combined EC method illustrates that temporal averaging alone might contribute to the general underestimation of turbulent fluxes.

The questions of which scales of coherent structures are typical for both sites and what spectra are measured by the Eddy Matrix remain open and should be investigated, e.g., using spectral analysis. Furthermore, it is not yet clear which time interval for the temporal covariance is best correlated with the spatial resolution of the spatial covariance and vice versa. An analysis of different interval lengths could answer that question. The spatial approaches used in this study also still need to be validated for other sites and longer data records covering a larger variability in weather conditions, but they already indicate some limits of Taylor's hypothesis. Therefore, when discussing systematic underestimation of turbulent fluxes by the EC method, the assumptions associated with Taylor's hypothesis need to be taken into account.

Acknowledgments In Namibia, the experiment profited significantly from the local support of the Gobabeb Research and Training Centre and of the University of Basel. The net radiation and soil heat flux data at

Gobabeb were provided by Dr. R. Vogt (University of Basel, Institute of Meteorology, Climatology and Remote Sensing) as part of his long-term cooperation with Gobabeb. This study would not have been possible without the engineering skills and understanding of U. Eichelmann, who constructed the unique set-up of the Eddy Matrix and perfectly synchronized the three data loggers under field conditions. Discussions with and advice from Dr. R. Vogt during the measurement campaign in Gobabeb in 2012 and during the finalization of the manuscript, in addition to comments from Dr. R. Queck (Institute of Hydrology and Meteorology, TU Dresden), are very much appreciated, as is support from TU Dresden.

References

Aubinet M, Vesala T, Papale D (2012) Eddy covariance: a practical guide to measurement and data analysis. Springer Science & Business Media, Berlin 438 pp

Chen J, Hu Y, Yu Y, Lü S (2014) Ergodicity test of the eddy correlation method. Atmos Chem Phys 14(12):18,207–18,254

Christen A, Vogt R (2004) Direct measurement of dispersive fluxes within a cork oak plantation. In: Proceedings of 26th conference on agricultural and forest meteorology, American Meteorological Society, 23–27 Aug 2004, Vancouver, BC, Canada

Desjardins RL, Schuepp PH, MacPherson JI, Buckley DJ (1992) Spatial and temporal variations of the fluxes of carbon dioxide and sensible and latent heat over the FIFE site. J Geophys Res 97(D17):18,467–18,475

Foken T (2008a) The energy balance closure problem: an overview. Ecol Appl 18(6):1351–1367

Foken T (2008b) Micrometeorology. Springer Science & Business Media, Berlin 306 pp

Frühauf C (1998) Verdunstungsbestimmung von Wäldern am Beispiel eines hundertjährigen Fichtenbestandes im Tharandter Wald. Tharandter Klimaprotokolle 1. Eigenverlag der Technischen Universität Dresden. Dissertation, TU Dresden, 185 pp

Kanda M, Inagaki A, Letzel MO, Raasch S, Watanabe T (2004) LES study of the energy imbalance problem with eddy covariance fluxes. Boundary-Layer Meteorol 110(3):381–404

Katul G, Hsieh CI, Bowling D, Clark K, Shurpali N, Turnipseed A, Albertson J, Tu K, Hollinger D, Evans B (1999) Spatial variability of turbulent fluxes in the roughness sublayer of an even-aged pine forest. Boundary-Layer Meteorol 93(1):1–28

Liu H, Peters G, Foken T (2001) New equations for sonic temperature variance and buoyancy heat flux with an omnidirectional sonic anemometer. Boundary-Layer Meteorol 100(3):459–468

Mahrt L (1998) Flux sampling errors for aircraft and towers. J Atmos Ocean Technol 15(2):416–429

Mahrt L (2010) Computing turbulent fluxes near the surface: needed improvements. Agric For Meteorol 150(4):501–509

Mahrt L, Thomas CK, Prueger JH (2009) Space-time structure of mesoscale motions in the stable boundary layer. Q J R Meteorol Soc 135(638):67–75

Mauder M, Desjardins RL, Pattey E, Gao Z, van Haarlem R (2008) Measurement of the sensible eddy heat flux based on spatial averaging of continuous ground-based observations. Boundary-Layer Meteorol 128(1):151–172

Mauder M, Desjardins R, Pattey E, Worth D (2010) An attempt to close the daytime surface energy balance using spatially-averaged flux measurements. Boundary-Layer Meteorol 136(2):175–191

McMillen RT (1988) An eddy correlation technique with extended applicability to non-simple terrain. Boundary-Layer Meteorol 43(3):231–245

Moore CJ (1986) Frequency response corrections for eddy correlation systems. Boundary-Layer Meteorol 37(1–2):17–35

Oncley SP, Foken T, Vogt R, Kohsiek W, DeBruin HAR, Bernhofer C, Christen A, Van Gorsel E, Grantz D, Feigenwinter C, Lehner I, Liebethal C, Liu H, Mauder M, Pitacco A, Ribeiro L, Weidinger T (2007) The energy balance experiment EBEX-2000. Part I: overview and energy balance. Boundary-Layer Meteorol 123(1):1–28

Panin GN, Tetzlaff G, Raabe A (1998) Inhomogeneity of the land surface and problems in the parameterization of surface fluxes in natural conditions. Theor Appl Climatol 60(1–4):163–178

Prescher AK, Grünwald T, Bernhofer C (2010) Land use regulates carbon budgets in eastern Germany: from NEE to NBP. Agric For Meteorol 150(7):1016–1025

Raupach MR, Shaw RH (1982) Averaging procedures for flow within vegetation canopies. Boundary-Layer Meteorol 22(1):79–90

Reynolds O (1895) On the dynamical theory of incompressible viscous fluids and the determination of the criterion. Philos Trans R Soc 186:123–164

Schotanus P, Nieuwstadt FTM, De Bruin HAR (1983) Temperature measurement with a sonic anemometer and its application to heat and moisture fluxes. Boundary-Layer Meteorol 26(1):81–93

Stoy PC, Mauder M, Foken T, Marcolla B, Boegh E, Ibrom A, Arain MA, Arneth A, Aurela M, Bernhofer C (2013) A data-driven analysis of energy balance closure across FLUXNET research sites: the role of landscape scale heterogeneity. Agric For Meteorol 171:137–152

Stull RB (1988) An introduction to boundary layer meteorology, vol 13. Kluwer Academic Publishers, Dordrecht 670 pp

Taylor GI (1938) The spectrum of turbulence. Proc R Soc 164(919):476–490

Thomas CK, Kennedy AM, Selker JS, Moretti A, Schroth MH, Smoot AR, Tufillaro NB, Zeeman MJ (2012) High-resolution fibre-optic temperature sensing: a new tool to study the two-dimensional structure of atmospheric surface-layer flow. Boundary-Layer Meteorol 142(2):177–192

Tillman JE (1972) The indirect determination of stability, heat and momentum fluxes in the atmospheric boundary layer from simple scalar variables during dry unstable conditions. J Appl Meteorol 11:783–792

Twine TE, Kustas WP, Norman JM, Cook DR, Houser PR, Meyers TP, Prueger JH, Starks PJ, Wesely ML (2000) Correcting eddy-covariance flux underestimates over a grassland. Agric For Meteorol 103(3):279–300

Wilson K, Goldstein A, Falge E, Aubinet M, Baldocchi D, Berbigier P, Bernhofer C, Ceulemans R, Dolman H, Field C (2002) Energy balance closure at FLUXNET sites. Agric For Meteorol 113(1):223–243